applied sciences

MDPI

*Article*

# Analysis of the Effect of Ultra-Fine Cement on the Microscopic Pore Structure of Cement Soil in a Peat Soil Environment

**Jing Cao [1], Chenhui Huang [1,*], Huafeng Sun [1], Yongfa Guo [2], Wenyun Ding [2] and Guofeng Hua [3]**

[1] Faculty of Civil Engineering and Mechanics, Kunming University of Science and Technology, Kunming 650500, China; 20040130@kust.edu.cn (J.C.); sunhuafeng@stu.kust.edu.cn (H.S.)
[2] Kunming Survey, Design and Research Institute Co., Ltd. of CREEC, Kunming 650200, China; guoyf@ey.crec.cn (Y.G.); dingwy@ey.crec.cn (W.D.)
[3] Sichuan Xinguangjian New Materials Technology Co., Ltd., Chengdu 610000, China; scxgj002@163.com
* Correspondence: 20212210066@stu.kust.edu.cn

**Abstract:** Treating peat soil foundations around Dianchi Lake and Erhai Lake in Yunnan is a complex problem in practical engineering projects. Peat soil solely reinforced with ordinary cement (OPC) does not satisfy demand. This study aims to solidify soil to achieve better mechanical properties. The preparation of peat soil incorporates a humic acid (HA) reagent into cohesive soil, and cement and ultra-fine cement (UFC) are mixed by stirring to prepare cement soil samples. They are then immersed in fulvic acid (FA) solution to simulate cement soil in the actual environment. X-ray diffraction (XRD), mercury intrusion porosimetry (MIP), scanning electron microscopy (SEM), and pores and cracks analysis system (PCAS) tests are used to study the impact of the UFC on the microscopic pore structure of cement soil in a peat soil environment. The unconfined compressive strength (UCS) test is used for verification. The microscopic test results indicate that incorporating UFC enhances the specimen's micropore structure. The XRD test results show the presence of C–S–H, C–A–S–H, and C–A–H. SEM and PCAS tests show that the UFC proportion increases by between 0% and 10%, and the percentage reduction in the macropore volume is the largest, at 38.84%. When the UFC admixture is 30%, the cumulative reduction in the percentage of macropore volume reaches 71.55%. The MIP test results show that the cumulative volume greater than 10 μm in pore size decreases from 7.68% to 0.17% with an increase in the UFC proportion. The UCS test results show that the maximum strength growth of cement soil is 12.99% when the UFC admixture is 0–10%. Incorporating UFC to form a compound curing agent solves the problem of the traditional reinforcement treatment of peat soil foundation being undesirable and decreases the amount of cement. This study provides practical guidance for reducing carbon emissions in actual projects.

**Keywords:** compound curing agent; pore structure; micro tests; macromechanical properties

check for updates

**Citation:** Cao, J.; Huang, C.; Sun, H.; Guo, Y.; Ding, W.; Hua, G. Analysis of the Effect of Ultra-Fine Cement on the Microscopic Pore Structure of Cement Soil in a Peat Soil Environment. *Appl. Sci.* **2023**, *13*, 12700. https://doi.org/10.3390/app132312700

Academic Editor: Kambiz Vafai

Received: 2 October 2023
Revised: 13 November 2023
Accepted: 18 November 2023
Published: 27 November 2023

**Copyright:** © 2023 by the authors. Licensee MDPI, Basel, Switzerland. This article is an open access article distributed under the terms and conditions of the Creative Commons Attribution (CC BY) license (https://creativecommons.org/licenses/by/4.0/).

## 1. Introduction

China's rapid economic development and industrialization have led to a short supply of quality land with better engineering properties; therefore, developing and utilizing soft soils and other poor foundation soils, such as peat soil foundations, has attracted attention. Peat soil (a collective term for peat and peaty soil) is a particular soft soil with a low natural weight, large porosity ratio, high compressibility, low bearing capacity, significant water content, high organic matter content, and low permeability [1,2]. The bad characteristics of peat soil introduce a complex problem during foundation reinforcement treatment. China has used cement to reinforce soft soils since the 1970s [3]. However, many engineering projects show that ordinary cement is used to reinforce peat soil with considerable organic matter content, and the strength of cement–solidified soil often fails to meet the design demands. Its mechanical properties are worse, making the reinforcement effect unsatisfactory. The fundamental reason is that the HA in peat soil engages in a sequence of physicochemical reactions with the hydration products in ordinary cement,

which are partially consumed, thus weakening its cementation and filling effects. The microstructure of cement soil produces many defects, leading to ordinary cement's failure to better exert its curing effect [4–7]. Liang S et al. [8] added HA to Nansha silt soil and cured it for different periods to study the effect of the organic matter mass fraction and curing age on the strength of organic silt soil. The results indicated that the presence of organic matter can hinder the hydration reaction in cement.

The effect of organic matter content on the strength of cement soil was limited and the decrease in cement soil strength became inconspicuous when the organic matter content was more than 5%. Cao J. et al. [9] immersed cement soil containing HA in an FA solution to study the effect of HA erosion on cement soil. The results indicated that an increased HA admixture reduced cement strength gradually, and the cement soil strength increased with the increase in immersion time. FA improved the initial cement soil's strength. A higher cement mixing ratio resulted in a more evident enhancement effect. Haitao L et al. [10] investigated the mechanical characteristics and microstructure of red clay containing organic matter cured with cement using cohesion, angle of internal friction, strength, and microscopic tests. The results indicated that cement soil's internal friction angle and strength decreased gradually with increasing organic matter content. The strength gradually approached a fixed value as it decreased. The fixed value was called the limit value, and the increase in organic matter content had little effect on the strength of the specimen once the limit value was exceeded. The cohesive force increased with the increase in organic matter content, and the presence of organic matter affected the formation of cement hydration products. Numerous scholars have studied peat soil sites, but more effective and environmentally friendly reinforcement materials are also being sought. This study introduces updated research results in the field of high–performance concrete to solve the above problems. Due to its excellent properties, UFC reduces the disadvantageous impacts of HA on the hydration products and the impact of external corrosion medium on the internal pore structure of the specimen and improves its macromechanical properties. People are seeking composite materials that reduce cement consumption and improve the mechanical properties of the solidified body in the context of global energy saving and emission reduction; therefore, this study has a high theoretical value and practical guiding significance for practical engineering projects.

The mechanical properties of cement-based materials are affected by many factors, including fineness, particle size, curing conditions, adhesive material type, and temperature [11–13]. Many scholars have studied cement-based materials' physical and chemical properties under different curing conditions by adding slag, fly ash, metakaolin waste, nanomaterials, and other materials and used SEM/EDX, XRD, TGA/DTG, resistivity, and other test methods to verify and analyze the unconfined compressive strength, viscosity value, yield strength, and other macromechanical properties of the enforcement [14–17]. In this experiment, the particle size distribution in the composite curing agent was improved by adding UFC. A higher Blaine area and smaller particle diameter of cement accelerated cement's hydration rate and strength development [18]. Improving cement particle fineness and optimizing the particle size distribution, type, and content of compound curing agents improved cement soil's mechanical properties. At the same time, the external admixture of UFC abandons the idea of traditional peat soil treatment with high organic matter content. In the context of global energy conservation and emission reduction, increasing the amount of cement or changing the type of cement to improve its strength is contradictory. In this study, the partial replacement of OPC with UFC increases the strength of cement soil and reduces the amount of cement. It is of great practical importance for China to achieve its carbon peaking and neutrality goals. Also, it can provide some ideas for the future treatment of different types of soft foundations. Li H J et al. [19] have shown that increasing the fineness of cement reduced the plastic viscosity of cement paste to a certain extent, significantly improved the early strength of cement paste, increased the hydration heat, advanced the peak of hydration heat, and shortened the induction period. The porosity of cement paste decreased with the increase in cement fineness. Kontoleontos F et al. [20] investigated the

impact of cement fineness on the physicochemical properties and microscopic structure of cement. The results indicated that fineness greatly influenced the early compressive strength. After 24 hours of hydration, the finer UFC's compressive strength was approximately three times that of OPC. The UFC showed a more compacted microstructure at the initial curing stage. At 28 days, macropores were partially filled with hydration products. After 28 days of hydration, the larger pores were in the 30–100 nm range, and the pore range of ordinary cement was in the 100–200 nm range. Aiqin W et al. [21] investigated the relationship between cement particle size distribution and cement properties. The results demonstrated that a narrow particle size distribution improved the hydration rate. The more extensive distribution index accelerated the hydration rate. Narrow distribution was advantageous in reducing the porosity of cement stone in the same water–cement ratio. Chen J et al. [22] investigated that UFC was an effective cementitious material to improve the performance of cement. The bulk density of cement and the fluidity, rheology, and strength of cement paste increased when the UFC was 10–20%. Arteaga–Arcos J C. et al. [23] introduced that UFC's incorporation improved cement particle distribution, optimized bulk density, and reduced porosity. The strength of the mortar is significantly improved when the UFC is 30~40%. Liu X et al. [24] used lime, gypsum, slag powder, UFC, and other parts to replace cement to form curing agents with different proportions and studied the early curing effect and failure characteristics of different proportions of curing agents on high water content soft soil. The results indicated that UFC greatly influenced the solidified soil strength, as the curing agent ratio was 20%. The solidified soil strength of 50% moisture was enhanced slowly as the UFC increased. There was a UFC threshold value.

The mechanical properties of cement soil fundamentally depend on its pore structure [25]. Due to the fine pore diameter, small number, uniform size distribution, and disconnected pores, the corrosive medium (acid, alkali, salt) does not susceptibly enter the pores and destroy the structure and distribution of pores. Its mechanical properties were less affected. Thus, exploring the micropore change mechanism of cement soil incorporating UFC helps to solve the problem of the undesirable traditional reinforcement treatment of peat soil foundations. Previous scholars' research has shown that adding admixtures improves the mechanical properties of cement-based materials. However, there is a lack of analysis of the samples' microscopic pore morphology, change form, and internal pore distribution. There was no more detailed analysis of the cement soil's internal pore structure. In this study, the results are verified by MIP, SEM, UCS, and other tests at the macro and micro levels. Finally, the influence mechanism of cement soil microstructure is proposed.

## 2. Experimental Program

### *2.1. Test Materials*

Figure 1 shows the experiment's apparent conditions of test soil, HA reagent, FA reagent, OPC, and UFC.




**Figure 1.** Test material diagram.

The fundamental state of the experimental materials is as follows:

(1) The test soil is the cohesive soil on the north slope of the student residence on the Chenggong Campus of Kunming University of Science and Technology. The brownish-yellow native soil has a low organic matter content, which has little effect on the experimental results. Table 1 shows the primary physical properties of the test soil. Figure 2a shows its microstructure. The soil particles are tightly connected with soil agglomerates (face-to-face connection) to form agglomerates with stronger cohesion. It appears irregular and granular, with the part planes relatively smooth and without significant unevenness, indicating its dense internal structure. Pores are barely visible.

**Table 1.** Chemical composition of the test soil and the mass fraction of each component.

| Test Soil | Chemical Composition and Their Contents (%) | | | | | | | | | | |
|---|---|---|---|---|---|---|---|---|---|---|---|
| | $SiO_2$ | $Fe_2O_3$ | $Al_2O_3$ | $TiO_2$ | $K_2O$ | MgO | CaO | $Na_2O$ | MnO | $P_2O_5$ | Ignition Loss |
| Cohesive soil | 46.57 | 21.22 | 20.8 | 8.9 | 0.48 | 0.48 | 0.16 | 0.04 | 0.14 | 0.57 | 0.64 |

(2) The Tianjin Guangfu Chemical Reagent Factory's (Tianjin, China) HA reagent is selected. The actual humic acid content is 41.68%, and Figure 2b shows its microstructure. The HA particles present irregular shapes. The connection between particles and particles, and particles and agglomerates, presents a weak dot–dot connection. HA presents interlinked pores and a spongy structure.

(3) Pingxiang Red Land Humic Group Co., Ltd. (Pingxiang, China) manufactures fulvic acid reagents with a 60% content. The microstructure is shown in Figure 3, and the fulvic acid agglomerate is colloidal.

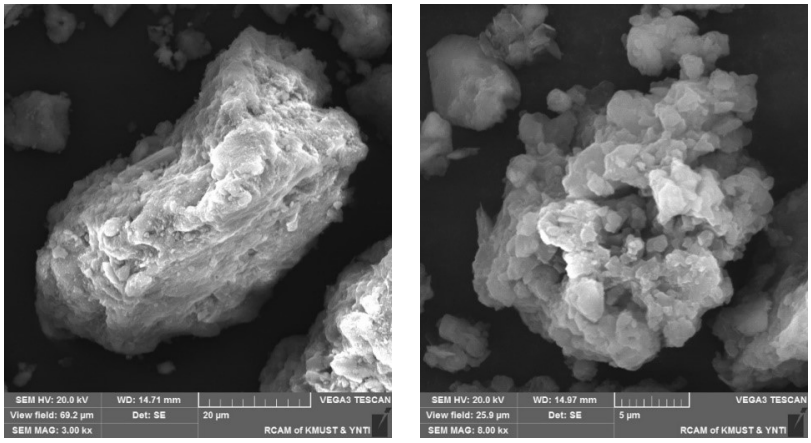
(4) Distilled water is used in both the FA solution and the preparation of the specimen in the test.

(5) The cement selection is selected from the Huaxin Cement Co., Ltd. (Kunming, China) produced by the Kunming Branch of Shilin P · O 42.5 Ordinary Portland Cement. Numerous scholars and engineers have researched the optimum cement mixing ratio for cement-reinforced soils in general soils and concluded that the most economical cement mixing ratio is about 12% [26]. However, the strength does not meet the demand of engineering construction for poor foundation soil with a high organic matter content at this cement mixing ratio. Through years of research, our group has found that the strength of the reinforcement is high, and the reinforcing effect is noteworthy as the cement mixing ratio is 20% [9,27].

(6) UFC is prepared from the above cement by physical grinding. The UFC's Blaine area obtained is over 9000 $cm^2/g$. It has a larger Blaine area than ordinary cement, and its specific surface area is generally determined using the BET model [28,29]. Table 2 shows the physical properties of the test materials. Table 3 shows the main chemical components of the two kinds of cement. The comparative data analysis shows the two uniform primary chemical compositions and contents. Figure 4a shows the cumulative grain size distribution curve. Figure 4b shows the particle size distribution curve. The UFC particle size is in a smaller range.

**Table 2.** Physical properties of the test materials.

| Material Type | $D_{95}$/μm | Maximum Particle Size/μm | Blaine Area/($cm^2/g$) | Color |
|---|---|---|---|---|
| OPC | 77.16 | 138.04 | 7880 | Grey |
| UFC | 8.23 | 11.83 | 10,703 | Grey |
| Cohesive soil | 673.57 | 2187.7 | / | Brownish yellow |
| HA | 261.38 | 478.63 | / | Black |




(**a**) (**b**)

**Figure 2.** (**a**) Microstructure image of the cohesive soil aggregate [30]. (**b**) Microstructure images of the HA aggregate [30].

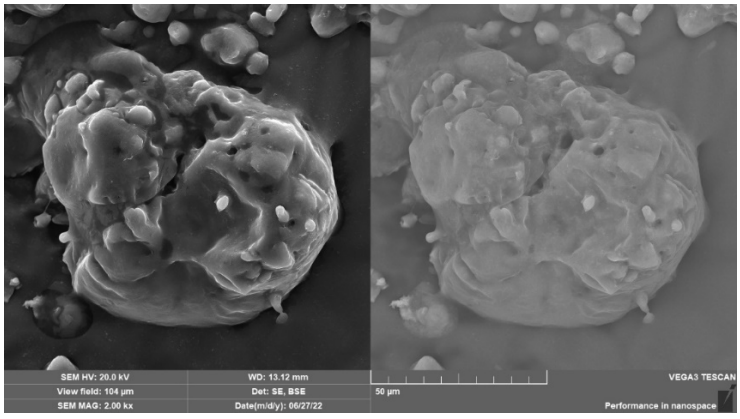
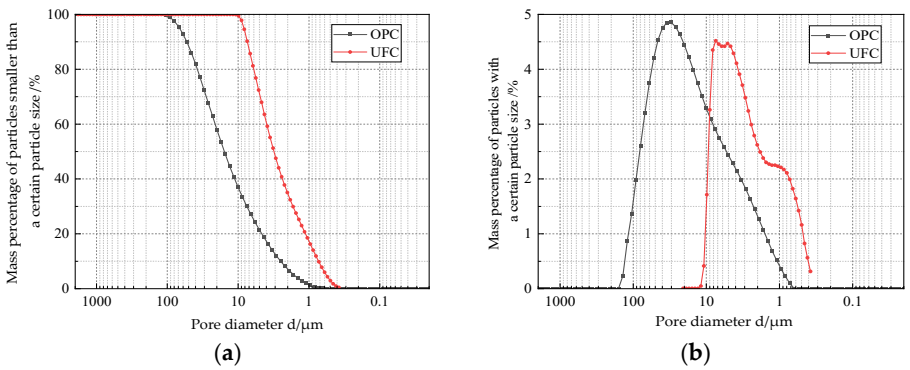



**Figure 3.** Microstructure image of the FA aggregate.

**Table 3.** Primary chemical composition of the cement curing agent.

| Material Category | Chemical Composition and Their Mass Fraction (%) | | | | | | | |
|---|---|---|---|---|---|---|---|---|
| | CaO | $SiO_2$ | $Al_2O_3$ | MgO | $Fe_2O_3$ | $Na_2O$ | $K_2O$ | Other |
| OPC | 65.5 | 18.4 | 5.3 | 3.9 | 2.9 | 0.5 | 0.3 | 3.2 |
| UFC | 65.5 | 18 | 5.4 | 3.8 | 2.9 | 0.5 | 0.3 | 3.6 |




(**a**) (**b**)

**Figure 4.** (**a**) The cumulative distribution curve of the OPC and UFC grain size gradation. (**b**) OPC and UFC grain size distribution curve.

### 2.2. Test Method and Specimen Preparation

The experiment controls the specimen ω = 24% moisture content and the void ratio e = 1.2. The cement mixing ratio is designed to be 20%, HA content is 15%, and the immersion solution's pH is 6.0. The UFC proportions are 0%, 10%, 20%, 30%, 40%, and 50%, and the immersion time is 90 days. Then, the specimens are tested and analyzed by the XRD test, MIP test, SEM test, PCAS micro semi-quantitative test, and UCS test. Table 4 shows the specific test design.

**Table 4.** Test design.

| Test Method | Cement Mixing Ratio β/% | UFC Proportion γ/% | HA Content λ/% | Moisture Content ω/% | Porosity Ratio /e | Soaking Liquid Category | Soaking Time /d |
|---|---|---|---|---|---|---|---|
| XRD, MIP, SEM, PCAS, UCS | 20 | 0<br>10<br>20<br>30<br>40<br>50 | 15 | 24 | 1.2 | FA solution (pH = 6.0) | 90 d |

According to the Standard for Geotechnical Testing Method (GB/T50123–2019) [31], the soil particles are sieved through a 2 mm sieve. The quality of raw materials is calculated according to Formulas (1)~(4), and cement soil is prepared by three-flap molds. The specimens are then placed in a curing box with a humidity of 95 ± 2% and a temperature of 20 ± 2 °C for ten days. After curing, the specimens are soaked in FA solution.

$$\lambda = \frac{m_{(HA)}}{m_{(soil)} + m_{(HA)}} \times 100\% \quad (1)$$

$$\beta = \frac{m_{(OPC)} + m_{(UFC)}}{m_{(soil)} + m_{(HA)}} \times 100\% \quad (2)$$

$$\gamma = \frac{m_{(UFC)}}{m_{(OPC)} + m_{(UFC)}} \times 100\% \quad (3)$$

$$m_{(water)} = (m_{soil} + m_{acid}) \times \omega \quad (4)$$

In the formulas: λ—HA content, %; $m_{(HA)}$—HA particulate quality, g; $m_{(soil)}$—soil particulate quality, g; β—cement mixing ratio, %; γ—UFC proportion; $m_{(OPC)}$—OPC quality, g; $m_{(UFC)}$—UFC quality, g; $m_{(water)}$—quality of distilled water in the specimen, g; ω—moisture content of the specimen, %.

### 2.3. Experimental Procedure

(1) XRD test

Preparation of the XRD specimen and experiment procedure: Firstly, the experimental group specimen is drawn out and then dried in an oven. An appropriate amount of specimen is placed in mortar to grind into powder, then passed through a 0.075 mm geotechnical sieve. A multifunctional powder X-ray diffractometer, Panacol X'Pert3 Powder, The Netherlands, determines the specimen's phases.

(2) MIP test

Preparation of the MIP specimen and experimental procedure: Firstly, the experimental group specimen is drawn out and then dried in an oven. Then, the specimens with a length, width, and height of 1 mm × 1 mm × 1 mm are cut at the same position. The specimens are then dried by the liquid nitrogen freezing vacuum sublimation drying method to remove water. Finally, pores in the cement soil are measured by an Autopore 9510 mercury porosimeter produced by the Micromeritics company. The pore diameter distribution of the specimen is achieved.

(3) SEM test

An SEM test is used to explore the micromorphological changes in UFC cement soil from a micro perspective. Preparation of the SEM specimen and experimental procedure: Firstly, the experimental group specimen is drawn out and then dried in an oven. The specimens with a length, width, and height of 30 mm × 20 mm × 15 mm are cut at the same position. The microstructure in the specimen is observed with a Czech TESCAN–VEGA3 fully automatic scanning electron microscope.

(4) PCAS test

PCAS preprocesses the SEM images and then extracts the corresponding microstructure parameter information through the microstructure processing program Pores and Cracks Analysis System (PCAS software, version number: V2.3) developed by the Department of Earth Science of Nanjing University. Finally, the pore distribution of cement soil specimens is statistically determined.

(5) UCS test

The UCS's macroscopic mechanical properties verify the microscopic analysis results. The UCS test is conducted with YSH–2 electric lime soil with no lateral limit compressive instrument produced by Nanjing Ningxi Soil Instrument Co., Ltd. (Nanjing, China) to determine the specimens' UCS with a 90 d immersion time. The arithmetic mean of the strength of the cement soil is the UCS. The test control instrument's axial compression rate was 1.0 mm/min.

The test procedure and specimen preparation are shown in Figure 5 [32–34].

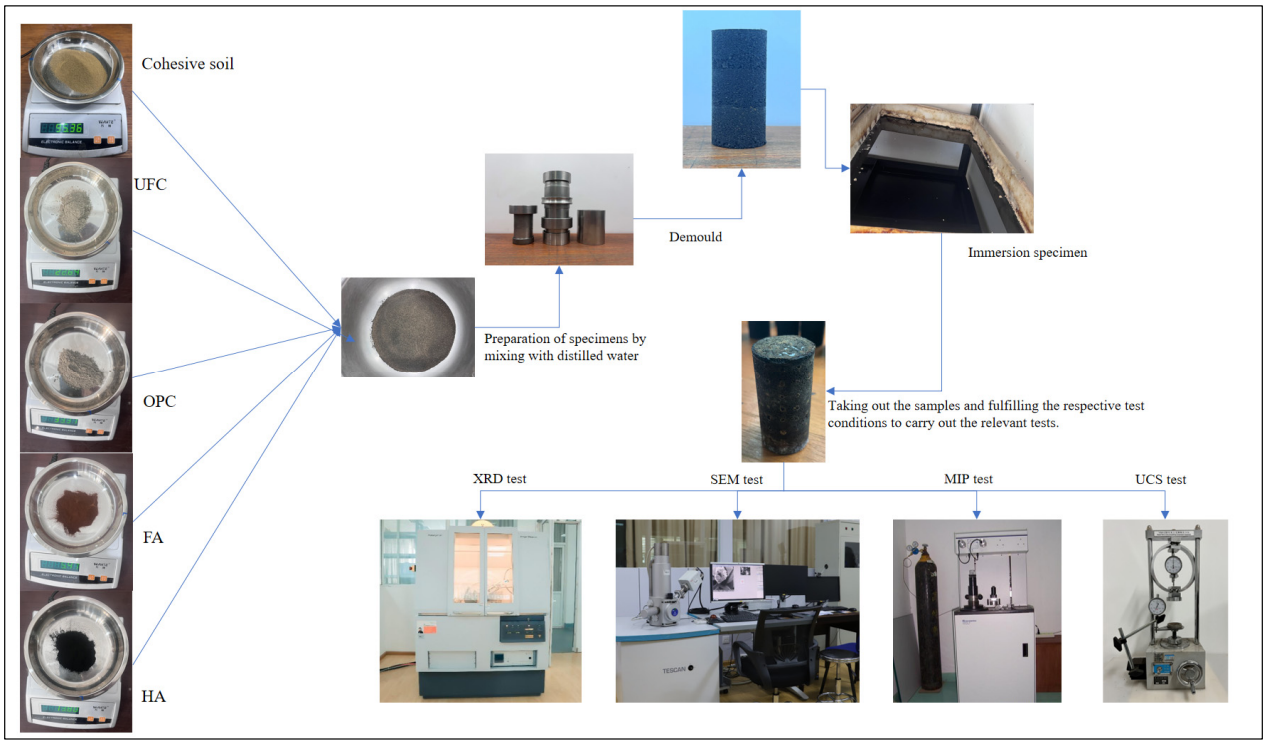



**Figure 5.** Test procedure.

## 3. Results and Analysis

### *3.1. Analysis of XRD Test Results*

Firstly, the XRD test is conducted on the test soil. The impact of incorporating UFC on the cement soil components is analyzed by accurately comparing the XRD test's results. Figure 6 shows the test results, and the major constituents of the test soil are (1) primary minerals: quartz ($SiO_2$) (ICDD–PDF:79–1906), mica ($KAl_2(AlSi_3O_{10})(OH)_2$) (ICDD–PDF:82–0576); (2) secondary minerals: kaolinite ($Al_2Si_2O_5(OH)_4$) (ICDD–PDF:78–1996). In addition

to the above minerals, there are Goethite (FeO (OH)) (ICDD–PDF:81–0462) and Anatase ($TiO_2$) (ICDD–PDF:21–1272).

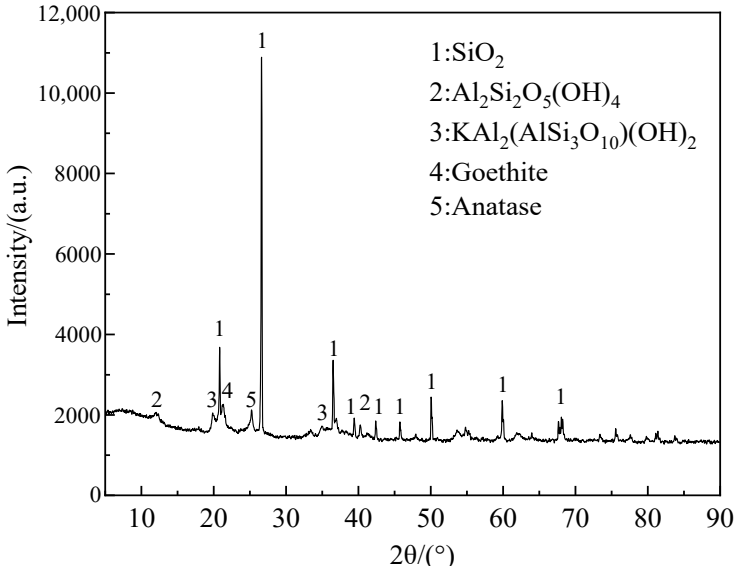



**Figure 6.** XRD pattern of the test soil (cohesive soil).

(a–f) in Figure 7 show the specimen's XRD patterns. (20% cement mixing ratio, 15% HA acid reagent content, pH = 6 FA solution, 90 d immersion time, 0%, 10%, 20%, 30%, 40%, 50% different UFC proportion). Its main components are primary minerals: quartz ($SiO_2$); secondary minerals: kaolinite ($Al_2Si_2O_5(OH)_4$), oxide ($TiO_2$); hydration product: calcium silicate hydrate (C–S–H) (ICDD–PDF:34–0002).

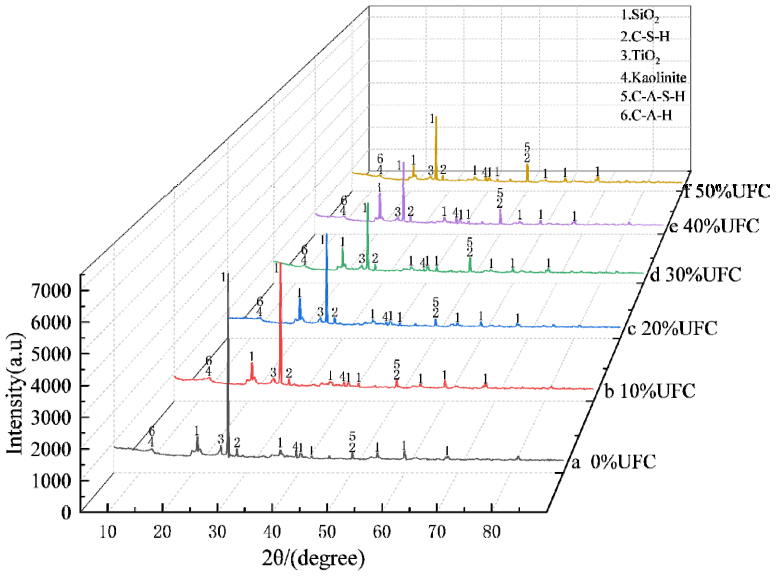



**Figure 7.** X-ray diffraction patterns of specimens with various UFC proportions (HA 15%, pH = 6.0, 90 d).

(a–f) in Figure 7 present the following phases by analysis. The related scholars' research results show that the cement's hydration product is mainly C–S–H. The diffraction angles 2θ corresponding to the XRD pattern are generally 29.1°, 31.8°, 49.8°, and 54.9° [35–38]. (a–c) in Figure 7 indicate that the XRD patterns show the presence of C–S–H, C–A–S–H(ICDD–PDF:18–0276), and C–A–H(ICDD–PDF:12–0408). As the UFC proportion increases, the present phases do not transform into other phases.

### 3.2. MIP Analysis of Test Results

Figure 8 is the pore and pore diameter distribution curve of cement soil (90 d immersion time, pH = 6.0 FA solution, 15% HA reagent content, 20% cement mixing ratio, 0%, 10%, 30%, 40%, and 50% UFC proportion). For the convenience of analysis, based on the curve characteristics in Figure 8, the pore diameter can be categorized into four classifications: (1) micropore d < 0.01 μm; (2) small pore 0.01 < d < 0.1 μm; (3) medium pore 0.1 < d < 10 μm; (4) macropore 10 μm < d < 100 μm. Figure 8a reveals that the distribution curve has three distinct peak-shaped distribution areas. The peak-shaped distribution area with a pore diameter of about 30 μm is the highest, followed by the peak-shaped distribution area with a pore diameter of about 2 μm and the lowest peak-shaped distribution area with a pore diameter of about 0.03 μm. The curve peak shows a downward trend with an increase in the UFC proportion, as the pore diameter is about 30 μm. The above indicates that the pore diameter percentage in cement soil between 10 μm and 100 μm decreases. When the UFC proportion is 50%, the macropores' percentage in the cement soil is almost zero. It indicates that the pore diameter of the macropores continues to decrease, and the connectivity of the macropores continues to decline. Thus, the macropores have been filled and transformed into smaller, close pores. The peak shows an upward trend with an increase in the UFC proportion as the pore diameter is approximately 2 μm. The above shows that the percentage of pore volume in the cement soil for pore diameters between 0.3 μm and 4 μm increases. The varying regularity of the pore diameter is similar between 0.01 μm to 0.1 μm and 0.3 μm to 4 μm.

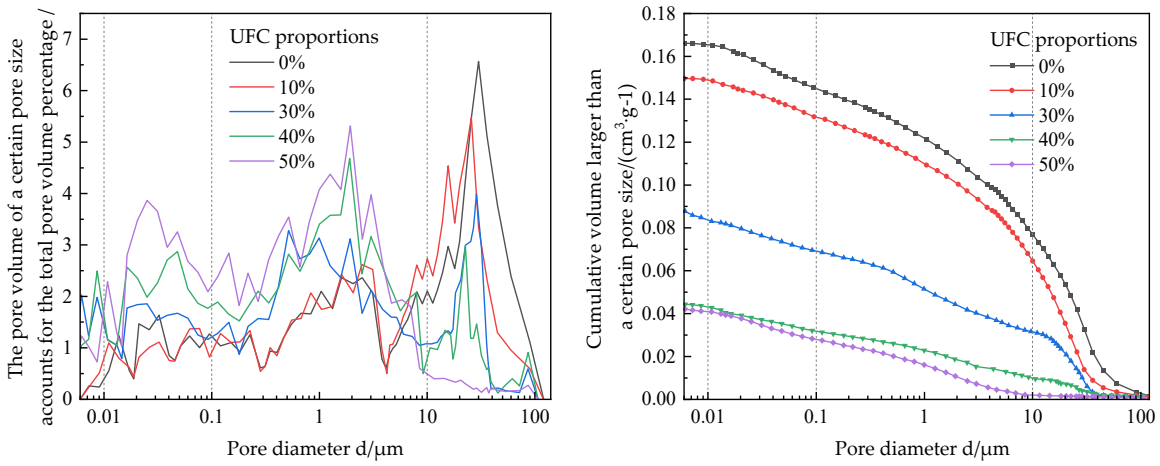



**Figure 8.** Pore diameter distribution curves of cement soil with different UFC proportions. (**a**) The distribution curve of pore volume percentage. (**b**) Accumulation curve of pore volume percentage greater than a certain diameter (HA 15%, pH = 6.0, 90 d).

In summary, the percentage of macropore volume in the cement soil shows a downward trend with an increase in the UFC proportion, and the percentage of medium and small pores volume presents a gradual upward trend. Increasing the UFC proportion improves the pore structure and enhances the compactness of the cement soil microstructure. The reason is that the macropores provide a larger space for hydration, and the cementitious products continuously cement the soil particles and fill pores. Hydration products fill the macropores preferentially as the UFC proportion increases, transforming into medium and small pores and increasing the volume percentage of medium and small pores in the cement soil.

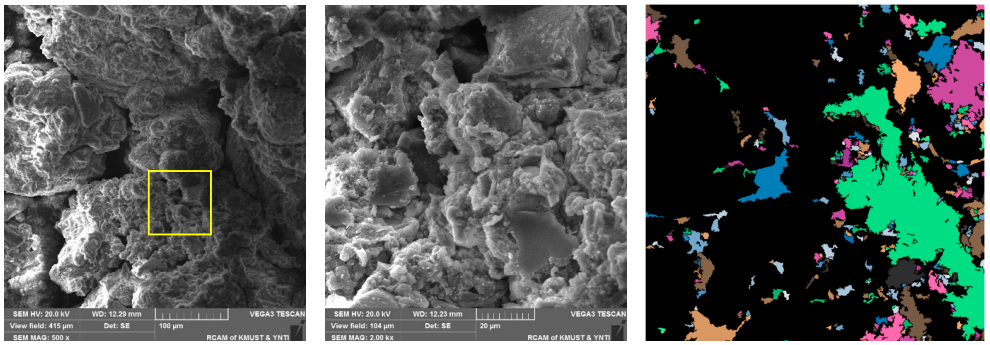
Figure 8b shows that the cumulative volume greater than 10 μm in pore size decreases from 7.68% to 0.17% with an increase in the UFC proportion. When the UFC proportion is less than 30%, the slope in the macropore range is steeper than that of the medium

and small pores. However, when the UFC proportion is greater than 30%, the slope in the macropore range gradually becomes gentle. The slope in the medium pore range is significant as the UFC proportion is less than 30%. After the UFC incorporation is more than 30%, the slope of the medium pore also tends to be gentle. The small pores and micropores show a relatively gentle trend. The pore diameter range of each pore decreases with an increase in UFC proportion. The specimens' internal pores have been filled with hydration products, the cement soil macropores have been refined, and the cement soil's internal pore morphology and structure have changed. This trend favors developing the macroscopic mechanical properties of cement soil from microscopic perspectives.

In summary, incorporating UFC decreases the percentage of macropores' volume in cement soil. Macropores gradually transform into medium and small pores. Both the pore volume distribution curves and cumulative pore volume curves are significantly lower. Analysis of mechanism: from the known hydration mechanism of ordinary silicates, the mechanism occurs in hydrolysis and hydration reactions of water with tricalcium silicate ($3CaO{\cdot}SiO_2$), dicalcium silicate ($2CaO{\cdot}SiO_2$), tricalcium aluminate ($3CaO{\cdot}Al_2O_3$), tetracalcium aluminoferrite ($4CaO{\cdot}Al_2O_3{\cdot}Fe_2O_3$), calcium sulfate ($CaSO_4$). The strength source of cement-based materials mainly comes from generating compounds, including aluminosilicate gel, calcium hydroxide, hydrous calcium silicate, hydrous calcium aluminate, and hydrous calcium ferrite through the above reactions. However, cement and its hydration products occur in serial physicochemical reactions with HA and FA in cement soil, affecting its reinforcing effect. Incorporating UFC to form a compound curing agent can regulate the hydration rate and degree of cement, generating more hydration products to a certain extent, weakening the influence of HA, and then achieving the purpose of the pore structure of denser cement soil. As shown in the above test results, incorporating UFC increases the proportion of fine particles in the compound curing agent, the curing agent's Blaine area, the hydration reaction rate, the hydration reaction extent, and the hydration products' quantity. These hydration products continuously cement particles and fill the interior pores, changing the connection mode of mineral aggregates and the pore structure of the cement soil. The macropores provide a larger space for the hydration reaction. They are pre-filled with hydration products as the UFC proportion increases. The macropores then transform into smaller medium and small pores, gradually increasing the percentage of medium and small pores' volume. This improvement is very beneficial for the strength and durability of cement soil. The significant reduction in the percentage of pore volume means that the distribution of pores is concentrated and uniform, there is a low probability of pore connectivity, and there is no longer an apparent connectivity of the pores. Finally, cement soil presents a denser and better-integrated microstructure.

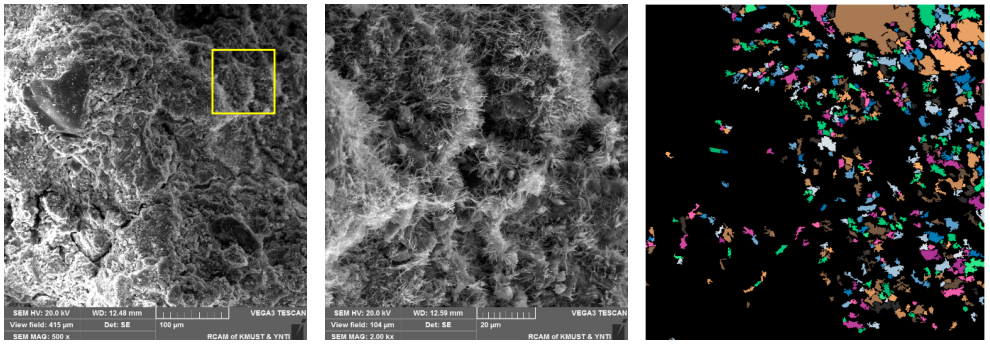
### *3.3. Analysis of SEM Test and PCAS Test Results*

SEM and PCAS tests are further conducted on cement soil specimens with various UFC proportions to explore the pore structure change in cement soil. It is the typical SEM image of cement soil specimens magnified 500 times and 2000 times. The microscopic pore segmentation images processed by PCAS software V2.3 are shown in Figure 9 (15% HA content, pH = 6 FA solution, 90 d immersion time, 0%, 10%, 20%, 30%, 50% UFC proportion). After the framed position in Figure 9a(1)–f(1) is enlarged 4 times, the 2000 times SEM image of Figure 9a(2)–f(2) is obtained. The SEM image (500 times) in Figure 9a(1)–f(1) is processed by PCAS software V2.3 to obtain the pore segmentation image in Figure 9a(3)–f(3).



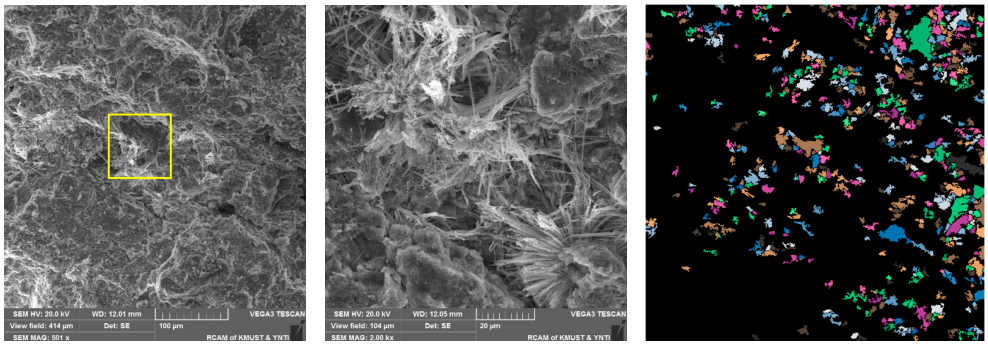
(1) (2) (3)

(**a**)



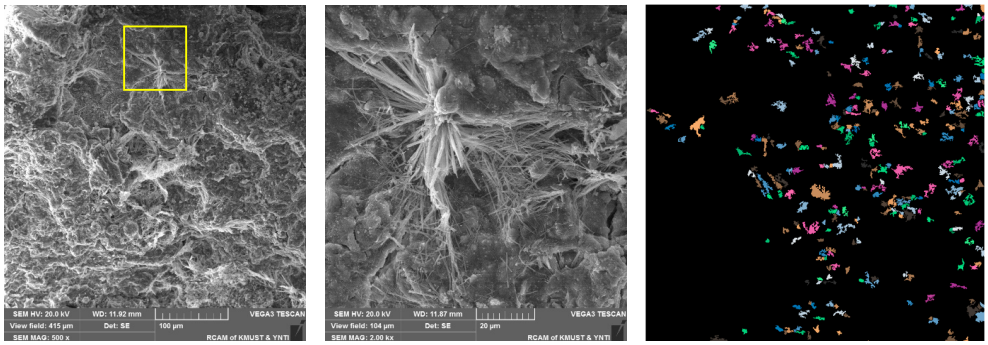
(1) (2) (3)

(**b**)



(1) (2) (3)

(**c**)



(1) (2) (3)

(**d**)

**Figure 9.** *Cont.*

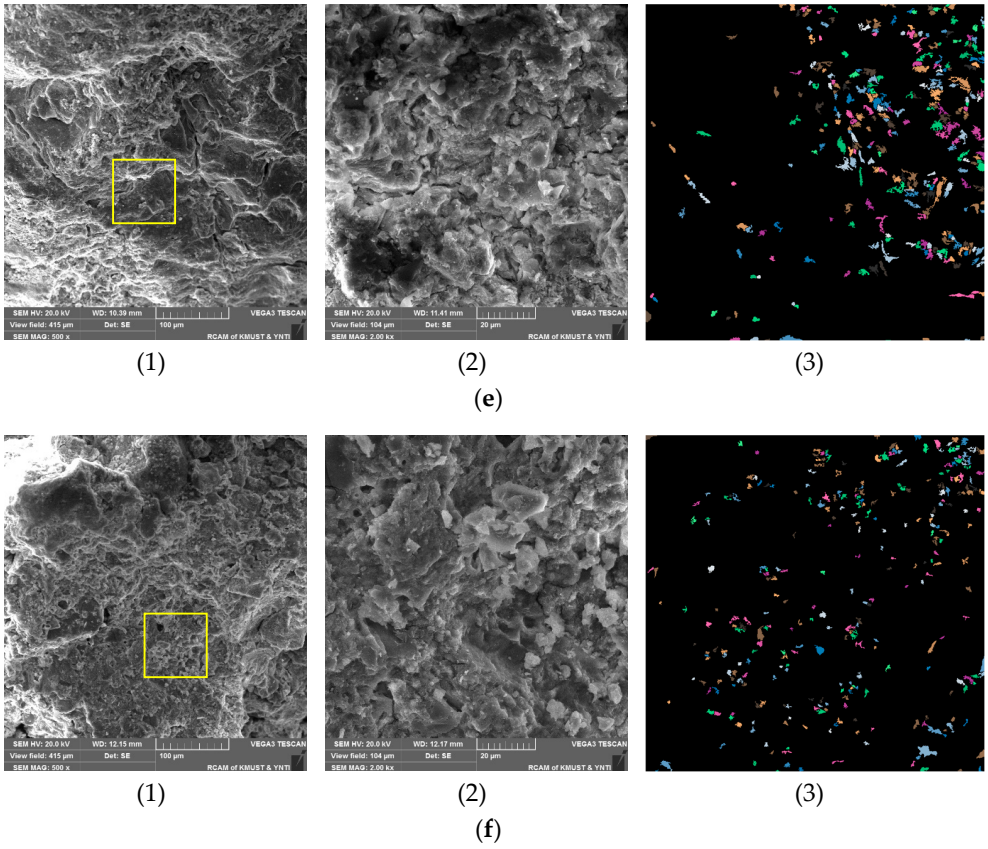



**Figure 9.** Microstructure images of cement soil with various UFC proportions [19] and PCAS pore segmentation processing images. (**a**) UFC proportion 0%. (**b**) UFC proportion 10%. (**c**) UFC proportion 20%. (**d**) UFC proportion 30%. (**e**) UFC proportion 40%. (**f**) UFC proportion 50%. (1) 500 times SEM image. (2) 2000 times SEM image of yellow frame. (3) PCAS pore segmentation image.

Figure 9a shows that the microstructure of the unadulterated UFC cement soil specimens exhibits evident aggregate–macropore–aggregate cohesion, and there are not enough hydration products wrapped and filled between aggregates. Thus, the pores of a larger overhead structure are formed in the cement soil. The skeleton of the cemented soil is loose, and the overall structural connection is feeble. In Figure 9b, the SEM image shows that the hydration products grow intricately on agglomerate surfaces and between pores. The fibrous hydration products are visible on them. There is a significantly reduced macropore, weakening the interconnectivity between the pores. The cement soil's overall structural cohesion is enhanced compared to the unadulterated UFC cement soil specimens. The fibrous and massive hydration products are visible, as shown in Figure 9c. The fibrous hydration products gradually accumulate and overlap to form massive hydration products, filling between aggregates and pores. There are further reduced macropores, further weakening the interconnectivity between pores. The cement soil forms a dense overall structure. Figure 9d–f show that the aggregates and pores are filled with hydration products, accumulating the hydration products in an orderly manner. The pore size is gradually invisible, and the pores are gradually disconnected. Cement soil forms a significantly denser overall structure, and its cohesion is powerful.

In summary, the UFC's incorporation gradually increases the relative content of hydration products. There is no sufficient hydration product between aggregates and pores, and hydration products gradually fill them. The hydration products accumulate from disorderly to orderly between the aggregates and the pores. The connectivity between pores changes from a large-area connection to a small-area connection to basically no

connection between pores. Its overall structure is from very loose to dense and presents as significantly denser.

PCAS can be used for the identification and semi-quantitative characterization of fractures and pores. The pore structure is analyzed by the pore data parameters obtained by PCAS. This experiment is only for macropores' analysis (pore diameter > 10 μm). The relationship curve of the macropores percentage and UFC proportion is shown in Figure 10. Figure 10 shows that the percentage of macropores' volume (pore diameter > 10 μm) shows an integrally downward trend with an increase in UFC proportion. The UFC proportion rises between 0% and 10%, and the reduction rate in the percentage of macropore volume is the largest, at 38.84%. When the admixture of UFC is 30%, the cumulative reduction in the percentage of macropore volume reaches 71.55%; however, when the admixture of UFC exceeds 30%, the reduction in the percentage of macropore volume gradually tends to level off. The above indicates that the hydration products continuously fill up the specimen's interior pores, which decreases the percentage of macropores' volume. The macropores gradually transform into enclosed medium and small pores, and the overall cohesion of the structure is enhanced. The results of the PCAS analysis are consistent with the results of the above MIP test. The comparison of the microtest results is shown in Table 5.

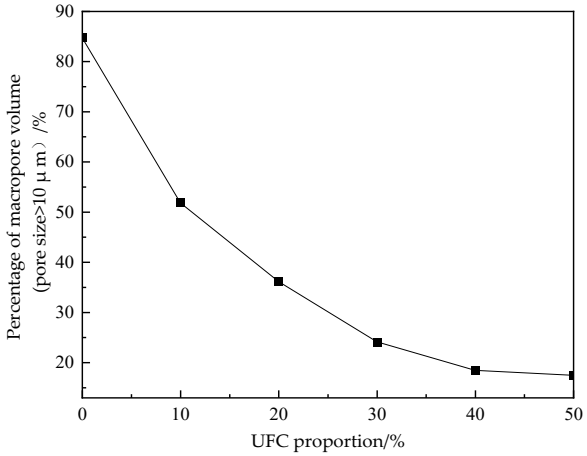



**Figure 10.** PCAS test results (percentage of macropore volume).

**Table 5.** Summary of microtests.

| XRD, MIP, SEM, and PCAS Comparison | |
|---|---|
| XRD test | The XRD patterns indicate the presence of hydration products, reflecting the many phases in the cement soil. |
| MIP test | The MIP test shows the change in the internal structure of the pores of the cement soil. With the increase in the UFC proportion, the macropores are transformed into small and medium pores, the cumulative pore volume percentage of large pores decreases, and the cumulative pore volume percentage of small and medium pores increases. |
| SEM test | The SEM test presents the number and morphological changes of hydration products and the changing forms of pores. As the UFC proportion increases, the number of hydration products increases and the lap hydration products are gradually ordered and flat. Fibrous hydration products gradually lap into massive hydration products—the pore space changes from visible to almost invisible. |
| PCAS test | The PCAS test demonstrates the connectivity of the internal pores' structure. With the increase in the UFC proportion, the internal structure of cement soil gradually changes from large-area connectivity to small-area connectivity. Finally, it shows that the pores are not connected. |

### *3.4. Analysis of UCS Test Result*

The curves of the strength related to the UFC proportion are given in Figure 11 (15% HA content, pH = 6 FA solution, 90 d soaking time.) The histogram of the strength growth

of specimens versus the immersion time for different UFC proportion ranges is given in Figure 12. The growth of the cement soil strength is 12.99%, 4.17%, 2.84%, 0.53%, and 1.74% for a UFC content of 0–10%, 10–20%, 20–30%, 30–40%, and 40–50%, respectively. From Figure 11 to Figure 12, it can be seen that the strength of the specimen increases continuously with an increase in the UFC proportion. Its strength growth is a maximum at 0–10% of the UFC proportion. The strength growth is slowed as the UFC proportion exceeds 10%. With the increase in the UFC proportion, the fine particles and Blaine area increase, the surface energy rises, and ultra-fine particles are unstable. The diameter of ultra-fine particles is small. The Van der Waals force between the particles is much larger than their gravity—part of the fine particles agglomerate reduces the comparative area of the agglomerate [30]. The surface reaction activity is reduced, the degree of hydration is lowered, and the amount of hydration products is reduced accordingly. The cement soil's strength development depends on the specimen's interior pore and the cementation between the hydration products and the cohesive soil agglomerates [39,40]. According to the above comprehensive microscopic test results, the proportion of gradually increased UFC increases the number of fine particles and Blaine area, promotes surface reaction activity, accelerates hydration reaction rate, promotes hydration's extent, and increases the hydration product's quantity. Cementation between soil agglomerates and hydration cementitious products constitutes the soil skeleton, and its cohesion is proportional to the number of hydration products. In the meantime, the specimen's interior pores are continuously filled with hydration products, changing the connection of mineral aggregates and the pore structure of the soil. The number of pores and the pore connectivity is reduced, the pore diameter distribution is uniform, the pore structure is refined, and the cement soil forms a relatively denser overall structure. The intrinsic reason for the gradual increase in cement soil strength depends on improving the compactness of the microscopic pore structure.

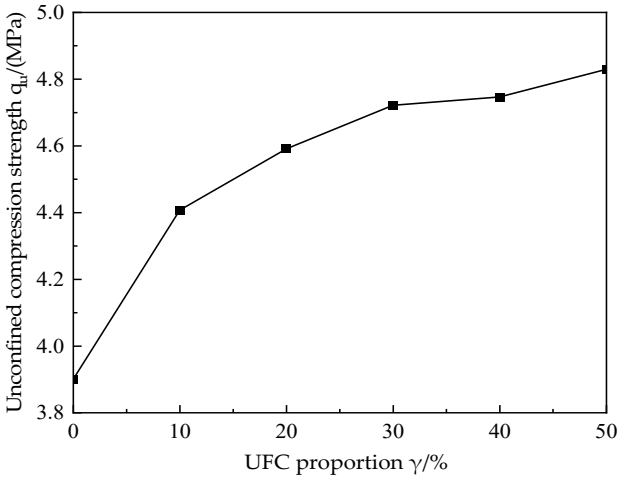



**Figure 11.** UCS curves of cement soil with various UFC proportions.

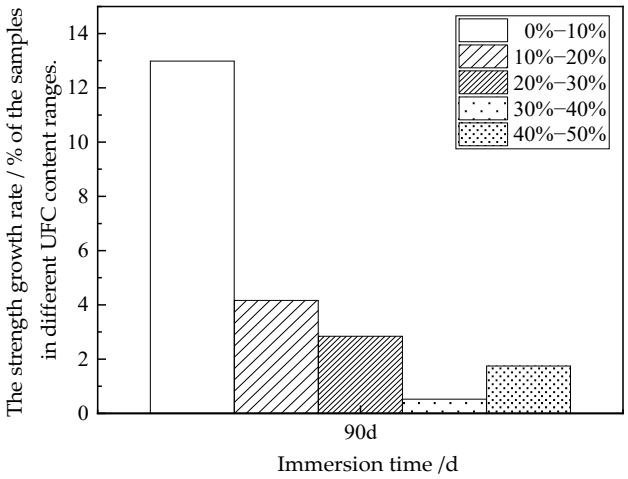



**Figure 12.** The strength growth rate of specimens within various UFC proportion ranges.

## 4. Conclusions

(1) The XRD patterns show the presence of C–S–H, C–A–S–H, and C–A–H.

(2) The MIP test results indicate that hydration products are gradually filled with the pores in the cement soil as the UFC incorporation increases. The pore morphology and structure in the cement soil are changed. The macropores gradually transform into medium and small pores. The percentage distribution curve and cumulative distribution curve of pores in cement soil are decreased. The cumulative volume greater than 10 μm in pore size decreases from 7.68% to 0.17% with an increase in the UFC proportion.

(3) The SEM and PCAS test results indicate that the UFC proportion rises between 0% and 10%. The reduction rate in the percentage of macropore volume is the largest, at 38.84%. When the admixture of UFC is 30%, the cumulative reduction in the percentage of macropore volume reaches 71.55%.

(4) The results of UCS tests indicate that the growth of cement soil strength is 12.99%, 4.17%, 2.84%, 0.53%, and 1.74% for a UFC proportion of 0–10%, 10–20%, 20–30%, 30–40%, and 40–50%, respectively. The strength growth is the maximum in the 0~10% proportion.

(5) The overall test results indicate that an increased UFC content improves cement soil's micropore structure and macro strength. In the future treatment of peat soil foundations, the conclusion of this paper can be combined to explore more valid methods to improve the cement soil in a peat soil environment. Decreasing the cement dosage promotes the sustainable development of society, providing practical guidance for decreasing $CO_2$ emissions in engineering.

**Author Contributions:** Conceptualization, J.C.; methodology, C.H.; software, Y.G.; validation, W.D.; formal analysis, C.H.; investigation, G.H.; data curation, H.S.; writing—original draft preparation, H.S.; writing—review and editing, C.H.; visualization, W.D.; supervision, Y.G.; project administration, G.H.; funding acquisition, J.C. All authors have read and agreed to the published version of the manuscript.

**Funding:** This research was funded by the Natural Science Foundation of China (Yunnan Province), grant number 41967035.

**Institutional Review Board Statement:** Not applicable.

**Informed Consent Statement:** Not applicable.

**Data Availability Statement:** The data used to support this study's findings are included in the article.

**Conflicts of Interest:** Author Yongfa Guo and Author Wenyun Ding were employed by the company Kunming Survey, Design and Research Institute Co., Ltd. of CREEC. Author Guofeng Hua was employed by the company Sichuan Xinguangjian New Materials Technology Co., Ltd. The remaining authors declare that the research was conducted in the absence of any commercial or financial relationships that could be construed as a potential conflict of interest.

## References


1. Liu, W.; Zhao, F.; Yang, W.; Chen, X. Features and properties of peaty soil in Caohai section of Anning-Sonming line. *Chin. J. Geotech. Eng.* **2013**, *35*, 671–674.
2. Wong, L.; Hashim, R.; Ali, F. Strength and permeability of stabilized peat soil. *J. Appl. Sci.* **2008**, *8*, 3986–3990. [CrossRef]
3. Zhang, S. The Infection on the Humic Acid in the Progress of Solidifying Soft Soil by Cement Soil. Ph.D. Thesis, Jilin University, Jilin, China, 2007.
4. Young, J. A review of the mechanisms of set-retardation in Portland cement pastes containing organic admixtures. *Cem. Concr. Res.* **1972**, *2*, 415–433. [CrossRef]
5. Zeng, W.; Tang, X.; He, M. Application of cement deep-mixing method in treatment of peat soil. *J. Geol. Hazards. Environ. Preserv.* **2002**, *13*, 67–69.
6. Thompson, M.R. Lime reactivity of Illinois soils. *J. Soil. Mech. Found. Div.* **1966**, *92*, 67–92. [CrossRef]
7. Chen, H. A Study on the Behavior of Organic Matter in the Progress of Solidifying Soft Soil by Cement. Ph.D. Thesis, Jilin University, Jilin, China, 2006.
8. Liang, S.; Zhou, J.; Luo, Q.; Lin, H. An Experimental Research on the Effect of Organic Matter on Mechanical Properties of Cementing Solidified Silt. *J. Guangdong Univ. Technol.* **2019**, *36*, 86–91.
9. Cao, J.; Song, Y.; Gao, Y. Preliminary experimental study on the corrosiveness of humic group to cement-soil. *J. Saf. Environ.* **2023**, *23*, 3098–3106.
10. Liu, H.; Xu, Z.; Shao, Z. Effect of Organic Matters on Mechanical Properties of Cement Treated Red Clay and its Micro-mechanism. *Soil. Eng. Found.* **2021**, *35*, 645.
11. Mohsen, A.; Kohail, M.; Alharbi, Y.R.; Abadel, A.A.; Soliman, A.M.; Ramadan, M. Bio-mechanical efficacy for slag/fly ash-based geopolymer mingled with mesoporous NiO. *Case Stud. Constr. Mater.* **2023**, *19*, e02283. [CrossRef]
12. Ramadan, M.; Kohail, M.; Abadel, A.A.; Alharbi, Y.R.; Soliman, A.M.; Mohsen, A. Exploration of mechanical performance, porous structure, and self-cleaning behavior for hydrothermally cured sustainable cementitious composites containing de-aluminated metakaolin waste and $TiO_2$ nanoparticles. *J. Mater. Res. Technol.* **2023**, *25*, 3998–4019. [CrossRef]
13. Ramadan, M.; Habib, A.; Kohail, M.; Mohsen, A. Enhancement of fresh and hardened properties of geopolymeric composite containing toxic lead sludge: A comparative study between the effect of superplasticizer and thermal treatment of sludge. *J. Build. Eng.* **2023**, *71*, 106482. [CrossRef]
14. Mohamed, O.; Hazem, M.; Mohsen, A.; Ramadan, M. Impact of microporous γ-$Al_2O_3$ on the thermal stability of pre-cast cementitious composite containing glass waste. *Constr. Build. Mater.* **2023**, *378*, 131186. [CrossRef]
15. Ramadan, M.; Kohail, M.; Alharbi, Y.R.; Abadel, A.A.; Binyahya, A.S.; Mohsen, A. Investigation of autoclave curing impact on the mechanical properties, heavy metal stabilization and anti-microbial activity of the green geopolymeric composite based on received/thermally-treated glass polishing sludge. *J. Mater. Res. Technol.* **2023**, *23*, 2672–2689. [CrossRef]
16. Essam, Y.; El-Faramawy, N.; Ramadan, W.; Ramadan, M. From dangerous wastes to green construction materials, as thermally stable-radiation blocker, in presence of meso-porous magnesia and alumina. *J. Build. Eng.* **2023**, *66*, 105896. [CrossRef]
17. Ramadan, M.; Habib, A.; Hazem, M.; Amin, M.; Mohsen, A. Synergetic effects of hydrothermal treatment on the behavior of toxic sludge-modified geopolymer: Immobilization of cerium and lead, textural characteristics, and mechanical efficiency. *Constr. Build. Mater.* **2023**, *367*, 130249. [CrossRef]
18. Wei, R.; Zeng, Y. The relationship between fineness and strength of different varieties of cement. *Cem. Eng. (Nanjing, China)* **1998**, 14–15.
19. Li, H.J.; Yang, L.; Xie, Y.J. Effect of fineness on the properties of cement paste. *Key Eng. Mater.* **2015**, *629*, 366–370. [CrossRef]
20. Kontoleontos, F.; Tsakiridis, P.; Marinos, A.; Katsiotis, N.; Kaloidas, V.; Katsioti, M. Dry-grinded ultrafine cements hydration. physicochemical and microstructural characterization. *Mater. Res. (Sao Carlos Braz.)* **2013**, *16*, 404–416. [CrossRef]
21. Aiqin, W.; Chengzhi, Z.; Ningsheng, Z. The theoretic analysis of the influence of the particle size distribution of cement system on the property of cement. *Cem. Concr. Res.* **1999**, *29*, 1721–1726. [CrossRef]
22. Chen, J.; Kwan, A. Superfine cement for improving packing density, rheology and strength of cement paste. *Cem. Concr. Compos.* **2012**, *34*, 1–10. [CrossRef]
23. Arteaga-Arcos, J.C.; Chimal-Valencia, O.A.; Yee-Madeira, H.T.; De La Torre, S.D. The usage of ultra-fine cement as an admixture to increase the compressive strength of Portland cement mortars. *Constr. Build. Mater.* **2013**, *42*, 152–160. [CrossRef]
24. Liu, X.; Wu, J. Study on the properties of curing agent material for soft soil with high water content. *J. Hunan Univ. Arts Sci. Nat. Sci. Ed.* **2019**, *31*, 85–89+94.
25. Valcuende, M.; Parra, C.; Marco, E.; Garrido, A.; Martínez, E.; Cánoves, J. Influence of limestone filler and viscosity-modifying admixture on the porous structure of self-compacting concrete. *Constr. Build. Mate.* **2012**, *28*, 122–128. [CrossRef]
26. Shao, Y. Study on Humus-Containning Soil Stabilization. Ph.D. Thesis, Zhejiang University, Zhejiang, China, 2006.

27. Song, Y.; Cao, J.; Ding, W.; Song, Z.; Liu, H.; Huang, S.; Zhu, W. Influence of Peat Soil Environment on Mechanical Properties of Cement-Soil and Its Mechanism. *Sustainability* **2023**, *15*, 4580. [CrossRef]
28. Wetwet, M.M.; El-Gamal, S.; Ramadan, M.; Hazem, M. Multifunctional cementitious blends containing zirconia nanoparticles: Mechanical characteristics, gamma attenuation behavior, and self-cleaning performance. *J. Build. Eng.* **2023**, *65*, 105736. [CrossRef]
29. Sayed, D.; El-Hosiny, F.; El-Gamal, S.; Hazem, M.; Ramadan, M. Synergetic impacts of mesoporous α-$Fe_2O_3$ nanoparticles on the performance of alkali-activated slag against fire, gamma rays, and some microorganisms. *J. Build. Eng.* **2022**, *57*, 104947. [CrossRef]
30. Cao, J.; Sun, H.; Huang, S.; Kong, C.; Liu, F.; Tian, L.; Zhu, W. Influence of ultrafine cement on cement-soil in peat soil environment of Dianchi Lake. *J. Civ. Environ. Eng.* **2023**.
31. *GB/T 50123-2019*; Standard for Geotechnical Testing Method. Ministry of Water Resources of the People's Republic of China. China Planning Press: Beijing, China, 2019.
32. Abo-El-Enein, S.; El-Hosiny, F.; El-Gamal, S.; Amin, M.; Ramadan, D.M. Gamma radiation shielding, fire resistance and physicochemical characteristics of Portland cement pastes modified with synthesized $Fe_2O_3$ and ZnO nanoparticles. *Constr. Build. Mater.* **2018**, *173*, 687–706. [CrossRef]
33. Ramadan, M.; Amin, M.; Sayed, M.A. Superior physico-mechanical, fire resistivity, morphological characteristics and gamma radiation shielding of hardened OPC pastes incorporating $ZnFe_2O_4$ spinel nanoparticles. *Constr. Build. Mater.* **2020**, *234*, 117807. [CrossRef]
34. Ramadan, M.; El-Gamal, S.; Selim, F. Mechanical properties, radiation mitigation and fire resistance of OPC-recycled glass powder composites containing nanoparticles. *Constr. Build. Mater.* **2020**, *251*, 118703. [CrossRef]
35. Chen, Y.; Zhong, H.; Yin, W.; Yao, G. Effect of Calcium–Silicon Ratio of Calcium Silicate Hydrate on Its Structure, Zeta Potential and Adsorption Capacity of Superplasticizer. *Bull. Chin. Ceram. Soc.* **2020**, *39*, 1798–1804.
36. Li, L.; Han, Q.; Yang, X.; Xiao, H.; Li, W.; Huang, S. Mechanical properties and micro-mechanisms of RHA-cement solidified sludge. *China. Civ. Eng. J.* **2022**. [CrossRef]
37. Lei, Y.; Han, T.; Wang, H.; Jin, X.; Yang, F.; Cao, H.; Cheng, F. Preparation and Characterization of Calcium Silicate Hydrate(C-S-H) Synthesized by the Hydrothermal Method. *Bull. Chin. Ceram. Soc.* **2014**, *33*, 465–469.
38. Cao, J.; Liu, F.; Huang, S.; Liu, H.; Song, Z.; Li, J.; Liu, G. Effect of UFC on the Microscopic Pore Structure of Cemented Soil in Humic Acid Environment. *Sustainability* **2023**, *15*, 3241. [CrossRef]
39. Huang, X.; Zhou, G. Harding Mechanism of Cement-Stablized Soil. *Chin. J. Geotech. Eng.* **1994**, *16*, 62–68.
40. Xun, Y. Test on strengthening soft soil with cementatory solidifying agent containing industrial waste. *Chin. J. Geotech. Eng.* **2000**, *22*, 210–213.


**Disclaimer/Publisher's Note:** The statements, opinions and data contained in all publications are solely those of the individual author(s) and contributor(s) and not of MDPI and/or the editor(s). MDPI and/or the editor(s) disclaim responsibility for any injury to people or property resulting from any ideas, methods, instructions or products referred to in the content.